Structural characterization of circuit configurations with purely imaginary eigenvalues[*]

Ricardo Riaza[†]

Departamento de Matemática Aplicada a las Tecnologías de la Información
Escuela Técnica Superior de Ingenieros de Telecomunicación
Universidad Politécnica de Madrid - 28040 Madrid, Spain
ricardo.riaza@upm.es

Caren Tischendorf[**]

Mathematisches Institut, Universität zu Köln
Weyertal 86-90, 50931 Köln, Germany
tischendorf@math.uni-koeln.de

Abstract

The hyperbolicity problem in circuit theory concerns the existence of purely imaginary eigenvalues (PIEs) in the linearization of the time-domain description of the circuit dynamics. In this paper we characterize the circuit configurations which, in a strictly passive setting, yield purely imaginary eigenvalues for all values of the capacitances and inductances. Our framework is based on branch-oriented, differential-algebraic circuit models which capture explicitly the circuit topology, and uses several notions and results from digraph theory. So-called *P-structures* arising in the analysis turn out to be the key element supporting our results. The analysis is shown to hold not only for classical (RLC) circuits but also for nonlinear circuits including memristors and other mem-devices.

Keywords: electrical circuit, oscillations, hyperbolicity, digraph, matrix pencil, differential-algebraic equation, memristor, memcapacitor, meminductor.

AMS subject classification: 05C50, 15A22, 34A09, 94C05, 94C15.

---

1   Introduction

Qualitative theory plays a key role in the analysis of nonlinear electrical and electronic circuits. Qualitative results are related e.g. to stability properties of equilibria and operating points [6, 16, 21, 27, 56], oscillations [12, 24, 36, 40], bifurcations [18, 38, 51] or chaotic phenomena [3, 4, 31, 32, 37, 46, 59, 61]. These references are just a sample of the huge literature addressing qualitative aspects in electrical and electronic engineering (cf. also [34] and references therein). Recent approaches are based on the use of semistate (differential-algebraic) circuit models, accommodating both nodal and hybrid techniques for setting up the circuit equations [8, 9, 15, 22, 47, 48, 49, 57, 58].

In this context, we extend in the present paper our previous research concerning qualitative properties of electrical circuits [52, 53] by focusing on the hyperbolicity problem. A linear time-invariant VIRLC circuit (that is, a circuit composed of independent voltage and current sources, and linear time-invariant resistors, inductors, and capacitors) is said to be *hyperbolic* if all the eigenvalues arising in the state-space description of the dynamics are away from the imaginary axis. Non-hyperbolic configurations exhibiting purely imaginary eigenvalues (PIEs) are important in linear circuit theory because they are responsible for proper oscillations. This problem is also relevant in the nonlinear context since purely imaginary eigenvalues may be responsible for Hopf bifurcations (see e.g. Example 3 in subsection 5.4 below) resulting in practice in nonlinear oscillations.

The research here reported is driven by two goals: first, we aim to extend the results of [53] by presenting a full characterization of so-called *topologically non-hyperbolic* configurations, which are those yielding purely imaginary eigenvalues for all positive values of the capacitances and inductances involved in the circuit. We refer the reader to subsection 2.3 for a more detailed description of this goal in terms of the equations which govern the circuit dynamics. Our second goal is to extend the hyperbolicity analysis to circuits with memristors and other mem-devices (memcapacitors and meminductors) [14, 29, 30, 33, 41, 43, 44, 45, 50, 54]; these devices, whose origin can be traced back to the 1971 paper [5] by Leon Chua, are taking a very relevant role in electronics, stemming from the report of the design of a nanometer memristor by HP in 2008 [55].

Our approach is based on the use of time-domain branch-oriented circuit models which capture explicitly the circuit topology; the differential-algebraic form of these models drives the spectral study to a matrix pencil setting. We will also make use of several concepts and results coming from digraph theory. All this material is compiled in Section 2. The first goal mentioned above is tackled in Section 3, where we extend the scope of the framework introduced in [53]; note that the results of [53] are restricted to circuits with one LC-loop or one LC-cutset only. Certain graph-theoretic structures (called *P-structures*) arising in the analysis will make it possible to extend those results to general circuits. Section 4 then revisits some examples from [53], trying not only to illustrate these notions and results but also to make it easier to read the proof of our main result, stated in Theorem 2. In Section 5 we extend the results to circuits with memristors, memcapacitors and meminductors, and additional examples are discussed. Finally, concluding remarks are compiled in Section 6.

2 Digraphs, circuit models, and the hyperbolicity problem

2.1 Some results from digraph theory

We compile below several notions and results from digraph theory which will be used in our analysis. Proofs and details can be found in [1, 2, 17]. We denote by b, n and c the number of branches, nodes and connected components in the digraph, respectively.

Cutsets and loops. A subset K of the set of branches of a digraph is a *cutset* if the removal of K increases the number of connected components of the digraph, and it is minimal with respect to this property, that is, the removal of any proper subset of K does not increase the number of components.

Given an orientation in every cutset, the cutset matrix $\bar{Q} = (q_{ij})$ is defined as

$$
q_{ij} = \begin{cases} 1 & \text{if branch } j \text{ is in cutset } i \text{ with the same orientation} \\ -1 & \text{if branch } j \text{ is in cutset } i \text{ with the opposite orientation} \\ 0 & \text{if branch } j \text{ is not in cutset } i. \end{cases}
$$

The rank of $\bar{Q}$ can be proved to be $n - c$; any set of $n - c$ linearly independent rows of $\bar{Q}$ defines a *reduced cutset matrix* $Q \in \mathbb{R}^{(n-c) \times b}$. In a connected digraph, any reduced cutset matrix has order $(n - 1) \times b$.

Analogously, given an orientation in every loop, the *loop matrix* $\bar{B}$ is defined as (b_{ij}), with

$$
b_{ij} = \begin{cases} 1 & \text{if branch } j \text{ is in loop } i \text{ with the same orientation} \\ -1 & \text{if branch } j \text{ is in loop } i \text{ with the opposite orientation} \\ 0 & \text{if branch } j \text{ is not in loop } i. \end{cases}
$$

This matrix can be shown to have rank $b - n + c$. A *reduced loop matrix* B is any $((b - n + c) \times b)$-submatrix of $\bar{B}$ with full row rank.

If the columns of the reduced loop and cutset matrices B, Q of a digraph are arranged according to the same order of branches, then $BQ^T = 0$, $QB^T = 0$. Moreover, the relations $\operatorname{im} Q^T = \ker B$ and $\operatorname{im} B^T = \ker Q$ do hold, and therefore the *cut space* $\operatorname{im} Q^T$ spanned by the rows of Q can be described as $\ker B$ and, analogously, the *cycle space* $\operatorname{im} B^T$ spanned by the rows of B equals $\ker Q$ (find details in [2]). The cut and cycle spaces are orthogonal to each other.

Lemma 1. *Let K be a subset of branches of a digraph. Then $\ker B_K$ and $\ker Q_K$ are spanned by maximal sets of independent K-cutsets and independent K-loops.*

This means that $\dim \ker B_k$ and $\dim \ker Q_K$ are defined by the number of independent K-cutsets and K-loops, respectively. In particular, K does not contain cutsets (resp. loops) if and only if B_K (resp. Q_K) has full column rank.

Blocks. A key role in our analysis will be played by certain subgraphs called *blocks*.

Definition 1. *A node is said to be an* articulation *if the removal of it and its incident branches increases the number of connected components of the digraph.*

Definition 2. *A digraph is said to be* non-separable *if it is connected and has no articulations.*

Definition 3. *A* block *is a maximal non-separable subgraph.*

For our purposes, the main property of blocks is the one stated below.

Lemma 2. *The branches of a block do not belong to any loop or cutset including branches from outside the block.*

Given a distinguished set of branches K, we will call a loop or cutset including elements from both K and $G - K$ a *hybrid* loop or cutset, respectively. Lemma 2 then says that the branches of a block K do not take part either in hybrid loops or in hybrid cutsets. The absence of hybrid loops can be seen as a direct consequence of the fact that two blocks can have at most one common vertex (see e.g. [1, Th. 1.13]), whereas the corresponding assertion for cutsets is explicitly stated in [1, Th. 3.23].

2.2 DAE models for nonlinear circuits

We will analyze in Sections 3 and 4 certain properties of (say, classical) electrical circuits composed of resistors, capacitors, inductors, and independent voltage and current sources; circuits with memristors and other mem-devices will be considered in Section 5. Provided that capacitors and resistors are voltage-controlled, and that inductors are current-controlled, the dynamics of a classical circuit can be described by the differential-algebraic system

$$C(v_c)v_c' = i_c \tag{1a}$$
$$L(i_l)i_l' = v_l \tag{1b}$$
$$0 = B_c v_c + B_l v_l + B_r v_r + B_j v_j + B_u v_s(t) \tag{1c}$$
$$0 = Q_c i_c + Q_l i_l + Q_r i_r + Q_j i_s(t) + Q_u i_u \tag{1d}$$
$$0 = i_r - \gamma(v_r), \tag{1e}$$

where $C(v_c)$ and $L(i_l)$ are the incremental capacitance and inductance matrices. For later use we denote the incremental conductance matrix $\gamma'(v_r)$ by $G(v_r)$. In (1) we are splitting the vectors of branch voltages and currents as $v = (v_c, v_l, v_r, v_j, v_s(t))$ and $i = (i_c, i_l, i_r, i_s(t), i_u)$, the subscripts c, l, r, j, u corresponding to capacitors, inductors, resistors, current sources and voltage sources, respectively. Note that for the voltage and current sources we use directly the explicit excitation terms $v_s(t)$, $i_s(t)$. Equations (1c) and (1d) express Kirchhoff's voltage and current laws in terms of the reduced loop and cutset matrices $B = (B_c \ B_l \ B_r \ B_j \ B_u)$, $Q = (Q_c \ Q_l \ Q_r \ Q_j \ Q_u)$ introduced above.

2.3 Linearization: the hyperbolicity problem

Let us now assume that all sources are DC ones (writing the excitation vectors as V_s and I_s) and fix the attention on an equilibrium point of (1), that is, a set of values for v and i which annihilates the right-hand side of (1). By letting C, L and G stand for the capacitance, inductance and conductance matrices at equilibrium, the linearization can be understood to govern the dynamics of the linear circuit described by the equations

$$
\begin{align}
Cv_c' &= i_c \tag{2a}\\
Li_l' &= v_l \tag{2b}\\
0 &= B_c v_c + B_l v_l + B_r v_r + B_j v_j + B_u V_s \tag{2c}\\
0 &= Q_c i_c + Q_l i_l + Q_r i_r + Q_j I_s + Q_u i_u \tag{2d}\\
0 &= i_r - G v_r. \tag{2e}
\end{align}
$$

In turn, the eigenvalues characterizing the dynamics of this circuit (and the local dynamics of (1) near equilibrium) are defined by the spectrum of the matrix pencil

$$
\begin{pmatrix}
\lambda C & 0 & -I & 0 & 0 & 0 & 0 & 0 \\
0 & -I & 0 & \lambda L & 0 & 0 & 0 & 0 \\
B_c & B_l & 0 & 0 & B_r & 0 & B_j & 0 \\
0 & 0 & Q_c & Q_l & 0 & Q_r & 0 & Q_u \\
0 & 0 & 0 & 0 & G & -I & 0 & 0
\end{pmatrix}, \tag{3}
$$

that is, the set of values of λ which makes the matrix in (3) a singular one; cf. [20, 49].

The eigenvalue analysis can be driven to the RLC setting by working with the so-called *reduced* circuit obtained after open-circuiting current sources and short-circuiting voltage sources. For an RLC circuit the dynamical behavior is defined by the system

$$
\begin{align}
Cv_c' &= i_c \tag{4a}\\
Li_l' &= v_l \tag{4b}\\
0 &= B_c v_c + B_l v_l + B_r v_r \tag{4c}\\
0 &= Q_c i_c + Q_l i_l + Q_r i_r \tag{4d}\\
0 &= i_r - G v_r, \tag{4e}
\end{align}
$$

the matrix pencil associated with (4) being

$$
\begin{pmatrix}
\lambda C & 0 & -I & 0 & 0 & 0 \\
0 & -I & 0 & \lambda L & 0 & 0 \\
B_c & B_l & 0 & 0 & B_r & 0 \\
0 & 0 & Q_c & Q_l & 0 & Q_r \\
0 & 0 & 0 & 0 & G & -I
\end{pmatrix}. \tag{5}
$$

Note that in (4) and (5), $B = (B_c \;\; B_l \;\; B_r)$ and $Q = (Q_c \;\; Q_l \;\; Q_r)$ are reduced loop and cutset matrices of the digraph which underlies the circuit obtained after open-circuiting current sources and short-circuiting voltage sources.

The pencil (3) or, equivalently, (5), and in turn the linear circuit models (2) and (4), are *hyperbolic* if they don't display purely imaginary eigenvalues $\lambda = \pm \omega j$. The chance to tackle the problem in the RLC setting is based on the following result, which is proved in [53].

Proposition 1. *Assume that a given VIRLC circuit has neither V-loops nor I-cutsets. The spectrum of the matrix pencil (3) coincides with that of the pencil (5), provided that the latter is defined by the RLC circuit obtained after open-circuiting current sources and short-circuiting voltage sources.*

Our goal in this paper will be to characterize the circuit configurations which lead to purely imaginary eigenvalues for all positive values of the capacitances and inductances, not only in the classical setting here described (our results in this context extending those presented in [53]) but also for circuits with mem-devices (cf. Section 5).

3 Topologically non-hyperbolic configurations in classical circuits

In light of (5) the analysis of non-hyperbolic circuit configurations involves looking for solutions λ of the form $\pm \omega j$ for the system

$$\lambda C v_c = i_c \tag{6a}$$
$$\lambda L i_l = v_l \tag{6b}$$
$$0 = B_c v_c + B_l v_l + B_r v_r \tag{6c}$$
$$0 = Q_c i_c + Q_l i_l + Q_r i_r \tag{6d}$$
$$0 = i_r - G v_r. \tag{6e}$$

Our results will focus on solutions $\lambda = \pm \omega j$ with $\omega \in \mathbb{R} - \{0\}$; see Theorem 1 below for the case $\lambda = 0$. Note also that, as far as resistors are strictly passive, the actual conductance values are known to be irrelevant (cf. Proposition 2 below). The analysis will be based on the following hypotheses.

Working hypotheses. *We will assume throughout Section 3 that the incremental capacitance and inductance matrices C and L are diagonal with positive entries, and that the incremental conductance matrix G is positive definite. Additionally, the circuits will have neither IC-cutsets (that is, cutsets formed just by current sources and/or capacitors) nor VL-loops (namely, loops defined by voltage sources and/or inductors only).*

A matrix M is positive definite if $u^T M u > 0$ for any non-vanishing real vector u we do not assume M to be symmetric. The assumptions on the circuit matrices mean that there is no coupling among reactive elements, and that all devices are strictly locally passive. In turn, the absence of IC-cutsets and VL-loops rules out zero eigenvalues (cf. Theorem 1 below). Note that IC-cutsets include in particular C-cutsets and, analogously, L-loops are particular instances of VL-loops; it is also worth remarking that open-circuiting the current sources in an IC-cutset leads to a C-cutset and, similarly, short-circuiting voltage sources within a VL-loop yields an L-loop.

3.1 Previous results

IC-cutsets and VL-loops define topologically non-hyperbolic configurations, since (for positive definite matrices C, L, G) they are known to characterize the existence of zero eigenvalues [25, 26, 39, 52, 53].

Theorem 1. *The matrix pencil (3) has a zero eigenvalue if and only if the circuit has at least one IC-cutset or one VL-loop.*

As stated in the working hypotheses above, we will preclude these configurations in order to focus the hyperbolicity analysis on the existence of non-zero, purely imaginary eigenvalues.

Eigenvectors associated with purely imaginary eigenvalues must necessarily have vanishing voltage and current in the resistor branches, as shown in Proposition 6 of [53] and stated below.

Proposition 2. *Any eigenvector associated with a PIE verifies $v_r = i_r = 0$.*

3.2 LC-blocks lead to PIEs

The following statement expresses a well-known property in circuit theory.

Proposition 3. *All eigenvalues of an LC-circuit are purely imaginary.*

Proof. In the absence of resistors, the pencil (5) reads

$$\begin{pmatrix} \lambda C & 0 & -I & 0 \\ 0 & -I & 0 & \lambda L \\ B_c & B_l & 0 & 0 \\ 0 & 0 & Q_c & Q_l \end{pmatrix}. \tag{7}$$

Assume that $(x_a^T, x_b^T, x_c^T, x_d^T) \neq 0$ is a left-eigenvector. This means that

$$\lambda x_a^T C + x_c^T B_c = 0 \tag{8a}$$
$$-x_b^T + x_c^T B_l = 0 \tag{8b}$$
$$-x_a^T + x_d^T Q_c = 0 \tag{8c}$$
$$\lambda x_b^T L + x_d^T Q_l = 0, \tag{8d}$$

and then

$$\lambda x_d^T Q_c C + x_c^T B_c = 0 \tag{9a}$$
$$\lambda x_c^T B_l L + x_d^T Q_l = 0. \tag{9b}$$

Let us multiply (9a) by $Q_c^T \overline{x_d}$; the transpose of the resulting equation, using the symmetry of C, is

$$\lambda x_d^* Q_c C Q_c^T x_d + x_d^* Q_c B_c^T x_c = 0. \tag{10}$$

7

Analogously, multiplying the conjugate of (9b) by $B_l^T x_c$ one gets

$$\overline{\lambda} x_c^* B_l L B_l^T x_c + x_d^* Q_l B_l^T x_c = 0. \tag{11}$$

Since $Q_c B_c^T + Q_l B_l^T = 0$, the sum of (10) and (11) yields

$$\lambda x_d^* Q_c C Q_c^T x_d + \overline{\lambda} x_c^* B_l L B_l^T x_c = 0. \tag{12}$$

The factors multiplying λ and $\overline{\lambda}$ are real because both C and L are symmetric. The real part of (12) then reads

$$\text{Re}\,\lambda (x_d^* Q_c C Q_c^T x_d + x_c^* B_l L B_l^T x_c) = 0. \tag{13}$$

Additionally, due to the fact that C and L are positive definite, the assumption $\text{Re}\,\lambda \neq 0$ would imply $x_d^T Q_c = 0$, $x_c^T B_l = 0$. In turn this would mean $x_c^T B_c = 0$, $x_d^T Q_l$ because of (9). Since both $(Q_c \;\; Q_l)$ and $(B_c \;\; B_l)$ have full row rank, we would derive $x_c^T = 0$, $x_d^T = 0$ which, together with $x_a^T = 0$, $x_b^T = 0$ from (8b) and (8c), lead to a contradiction since $(x_a^T, x_b^T, x_c^T, x_d^T)$ was supposed not to vanish. $\qquad \square$

Proposition 4. *Consider a VIRLC circuit. If after open-circuiting current sources and short-circuiting voltage sources there exists an LC-block, then the circuit has a PIE.*

This is an immediate consequence of Proposition 3 above and the decoupled structure of the pencil (7) in the presence of a block, since according to Lemma 2 a block displays no hybrid loops or cutsets. Note that an eigenvalue-eigenvector pair of the LC-block can be extended to an eigenvalue-eigenvector pair of the whole circuit just by setting the remaining entries in the eigenvector to zero.

3.3 Statement of the main result

The converse of Proposition 4 is not true: the examples discussed in [53] (cf. also Section 4 below) show that there are RLC circuits without LC-blocks displaying PIEs for certain values of the reactances. However, one may conjecture that if a circuit has PIEs for *all* positive values of the reactances, it must be because an LC-block is exhibited after open-circuiting current sources and short-circuiting voltage sources. This is a natural conjecture, but its proof turned out to be more difficult than expected. The remainder of Section 3 is devoted to show that this conjecture (stated as Theorem 2 below) is actually true.

Theorem 2. *A VIRLC circuit has a PIE for all positive values of capacitances and inductances if and only if, after open-circuiting current sources and short-circuiting voltage sources, the reduced circuit exhibits an LC-block.*

The "if" part is already stated in Proposition 4. We need to prove that the "only if" part is true. In the sequel we work with the reduced RLC circuit (that is, the circuit obtained after open-circuiting current sources and short-circuiting voltage sources) without further mention; note that the assumed exclusion of IC-cutsets and VL-loops precludes C-cutsets and L-loops in the reduced circuit.

3.4 P-structures

The key aspect in the proof of Theorem 2 emanates from the following remarks. In the light of Proposition 2, the eigenvalue-eigenvector equations (6) read

$$\lambda C v_c = i_c \tag{14a}$$
$$\lambda L i_l = v_l \tag{14b}$$
$$B_c v_c + B_l v_l = 0 \tag{14c}$$
$$Q_c i_c + Q_l i_l = 0, \tag{14d}$$

for which a solution $\lambda = \omega j \neq 0$ is assumed to exist for all positive values of C and L. Of course, the actual values of λ and ω will depend on C, L.

Fix a set of values for C and L, and focus on the non-vanishing entries of v_c, v_l, i_c and i_l within an associated eigenvector. Note that, from (14a) and (14b), exactly the same entries vanish in the voltage and the current vector. Additionally, not all v_l's (hence not all i_l's) can vanish since, otherwise, the equation $B_c v_c = 0$ resulting from (14c) would indicate the existence of a C-cutset (cf. Lemma 1). Analogously, not all i_c's (hence not all v_c's) may vanish since $Q_l i_l = 0$ from (14d) would signal an L-loop, using again Lemma 1.

Let K stand for the set of capacitive and inductive branches with non-vanishing voltage and current in the above-referred eigenvector. Use a subscript k to denote the corresponding (non-vanishing) entries of v_c, v_l, i_c and i_l, and also to specify the submatrices of B_c, B_l, Q_c and Q_l defined by the columns which correspond to K-branches, as well as the capacitances and inductances of the K-branches. With this notation, from (14) we get

$$\lambda C_k v_{ck} = i_{ck} \tag{15a}$$
$$\lambda L_k i_{lk} = v_{lk} \tag{15b}$$
$$B_{ck} v_{ck} + B_{lk} v_{lk} = 0 \tag{15c}$$
$$Q_{ck} i_{ck} + Q_{lk} i_{lk} = 0. \tag{15d}$$

The fact that all v_{ck} and v_{lk} within equation (15c) do not vanish indicate, in the light of Lemma 1, that every K-branch forms at least one cutset just with other K-branches. Indeed, since $(v_{ck}, v_{lk}) \in \ker(B_{ck}\ B_{lk})$, this vector can be written as a linear combination of vectors describing K-cutsets; additionally, every K-branch must have a non-vanishing entry in at least one of these vectors since, otherwise, the corresponding entry in v_{ck} or v_{lk} would vanish.

Proceeding analogously, (15d) indicates that every K-branch forms at least one loop just with other K-branches.

Definition 4. *A set K of capacitive and inductive branches, together with their incident nodes, is said to form a* P-structure *if every branch in K forms at least one cutset and at least one loop just with other branches from K.*

Examples of P-structures can be found in Figure 2 below. It is worth clarifying that the cutset and the loop arising in this definition do not need to include all the branches in K;

nor it must happen that the cutset and the loop involve the same branches. For the sake of terminological simplicity we will use K also to mean the subgraph defined by the K-branches and their incident nodes.

The "P" within the term "P-structure" comes from "PIE". This term, however, should not be erroneously understood to guarantee the existence of a PIE; it just reflects the fact that these structures are the candidates which may (but not necessarily do) support the existence of a PIE.

In the light of Definition 4, the discussion above indicates that the branches corresponding to the non-vanishing entries of an eigenvector associated with a PIE form a P-structure. Briefly, we will say that the PIE-eigenvector arises from this P-structure.

An LC-block which does not amount to a single branch can be checked to be a P-structure (note, incidentally, that the P-structures from which a PIE-eigenvector arises include at least two branches, namely a capacitor and an inductor). Certainly, the converse is not true. The proof of Theorem 2 is closely related to this fact. The idea of the proof is that the values of the capacitances and inductances of each P-structure, if it is not a block, must satisfy certain restrictions in order to allow for the existence of PIEs. Therefore, in order to have a PIE for all positive values of the capacitances and the inductances, at least one of these P-structures must be an LC-block. This is detailed in subsection 3.5 below.

Some instances of P-structures. The notion of a P-structure can be illustrated by means of the circuits in Figure 1, already analyzed in [53]. Both circuits have a unique P-structure, as displayed in Figure 2. In both cases the P-structure is defined by the four reactances. In the circuit depicted on the left, the four reactances define simultaneously a loop and a cutset. In the circuit on the right, there are two loops (defined by L_1, C_1 and by L_2, C_2, respectively) and just one cutset defined by the four reactances.
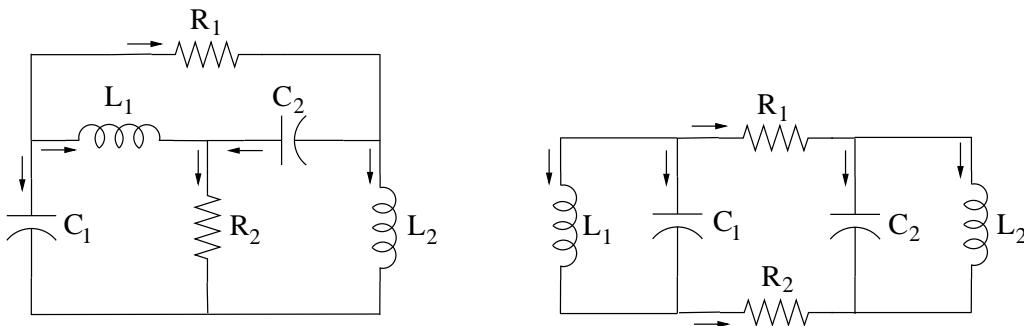

Figure 1: RLC circuits.

3.5 Proof of Theorem 2

Assume that (v_c, v_l, i_c, i_l) is an eigenvector associated with a PIE of an RLC circuit (possibly arising as the reduction of a VIRLC circuit in which current sources are open-circuited and
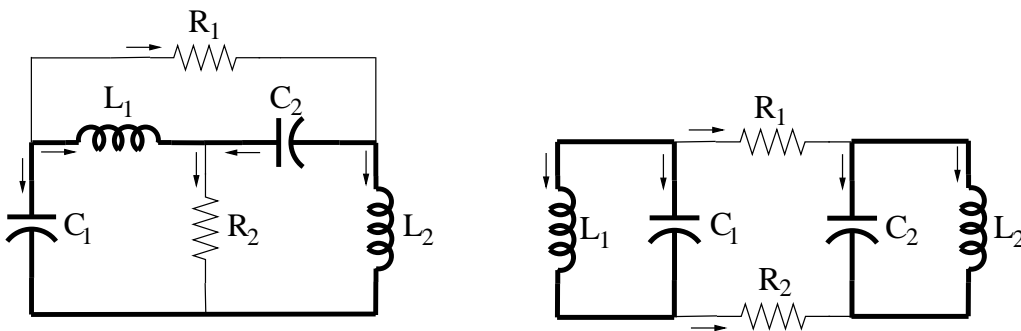
Figure 2: P-structures.

voltage sources short-circuited). Consider the associated P-structure K signaled by the non-vanishing entries of this eigenvector, and recall the relations depicted in (15). Let b_k, n_k and c_k stand for the number of branches, nodes and connected components of K.

Lemma 3. *If the P-structure K is not a block, then the rank of $B_k = (B_{ck} \ B_{lk})$ is greater than $b_k - n_k + c_k$; if it is a block then $\operatorname{rk} B_k = b_k - n_k + c_k$.*

Proof. Since K is a (sub)circuit, it has $b_k - n_k + c_k$ independent loops. Assume, without loss of generality, that the first rows of the original loop matrix B are defined from these $b_k - n_k + c_k$ independent loops.

Note that $B_k = (B_{ck} \ B_{lk})$ is a submatrix of B including entries from *all* of the rows, and that B_k has at least rank $b_k - n_k + c_k$ since the first $b_k - n_k + c_k$ rows are linearly independent. Write as $\tilde{B}_k$ the submatrix of B_k defined by the first $b_k - n_k + c_k$ rows, and note that this is a reduced loop matrix of the K-subcircuit.

Suppose that K is not a block; this means that there exists a hybrid loop (cf. Lemma 2), namely, a loop including some branches from K and some others (label them with Z) which are not in K. Such a hybrid loop can be used to define a row of B in a way such that the corresponding row of the submatrix B_k is linearly independent of the first $b_k - n_k + c_k$ ones. Assume it is not. Write the hybrid-loop row of B_k as a linear combination of the $b_k - n_k + c_k$ first ones. In the full B matrix, substract from the hybrid-loop row this linear combination, and note that the Z entries do vanish in the first $b_k - n_k + c_k$ rows. This results in an element of the cycle space which consists only of the Z-entries of the hybrid loop, but this is impossible since this would correspond to a "subloop" of the original hybrid loop.

This means that the existence of a hybrid loop makes the rank of the submatrix B_k greater than $b_k - n_k + c_k$. Hence, if the P-structure is not a block, then the rank is greater than $b_k - n_k + c_k$. Notice also that if K is a block, then the rank of B_k is $b_k - n_k + c_k$ because the remaining rows in B have zeros in the K-entries.

$\square$

Regarding the cutset matrix Q, notice that $\ker Q_k$ is spanned by linearly independent K-loops. Since the K-loops are the same in the original circuit and in the K-subcircuit, this

means that $\ker Q_k$ equals $\ker \tilde{Q}_k$, where $\tilde{Q}_k$ is any (reduced) cutset matrix of the K-circuit.

According to the construction in Lemma 3 above, the first $b_k - n_k + c_k$ rows of (15c) read $\tilde{B}_k v_k = 0$, where v_k stands for (v_{ck}, v_{lk}). Additionally, the above-mentioned identity $\ker Q_k = \ker \tilde{Q}_k$ means that (15d) can be recast as $\tilde{Q}_k i_k = 0$, the vector i_k standing for (i_{ck}, i_{lk}). This yields the following result.

Lemma 4. *A PIE of the original circuit is also a PIE of the corresponding K-subcircuit, the non-vanishing entries of the original eigenvector defining an eigenvector of the K-subcircuit.*

These properties make it possible to prove our main statement.

Proof of Theorem 2. The proof is crucially based on the fact that all PIE-eigenvectors must arise from some P-structure, according to Lemma 4.

Fix a P-structure K. We can choose the values of capacitances and inductances of the K-subcircuit in such a way that all eigenvalues of that subcircuit are simple. Moreover, this is true for parameter values lying on an open dense subset in $\mathbb{R}_+^{b_k}$, where b_k is the number of branches in K (and $\mathbb{R}_+$ is the set of positive real numbers). This is a consequence of the fact that eigenvalues are given by the roots of the polynomial defined by the determinant of (7), which has the form $p(\lambda, C, L) = a_m(C, L)\lambda^m + a_{m-1}(C, L)\lambda^{m-1} + \ldots + a_0(C, L)$. Note that $a_0(C, L) \neq 0$ because the absence of C-cutsets and L-loops rules out null eigenvalues. Multiple eigenvalues are defined by the intersection of $p(\lambda, C, L) = 0$ and $p_\lambda(\lambda, C, L) = 0$ and, therefore, occur only on a lower dimensional set of the parameter space. This means that the set of values of C_k, L_k for which all eigenvalues are simple is open and dense in $\mathbb{R}_+^{b_k}$, and implies that the corresponding branch equations have generically corank one, namely, that the coefficient matrix of

$$\lambda C_k v_{ck} = i_{ck} \tag{16a}$$
$$\lambda L_k i_{lk} = v_{lk} \tag{16b}$$
$$\tilde{B}_{ck} v_{ck} + \tilde{B}_{lk} v_{lk} = 0 \tag{16c}$$
$$\tilde{Q}_{ck} i_{ck} + \tilde{Q}_{lk} i_{lk} = 0 \tag{16d}$$

has generically corank one when $\lambda = \omega j$ is an eigenvalue of the K-subcircuit. Write the corresponding linear system as

$$
\begin{pmatrix}
\lambda C_k & 0 & -I & 0 \\
0 & -I & 0 & \lambda L_k \\
\tilde{B}_{ck} & \tilde{B}_{lk} & 0 & 0 \\
0 & 0 & \tilde{Q}_{ck} & \tilde{Q}_{lk}
\end{pmatrix}
\begin{pmatrix}
v_{ck} \\
v_{lk} \\
i_{ck} \\
i_{lk}
\end{pmatrix}
= 0. \tag{17}
$$

Now, for an eigenvalue of the K-subcircuit to be an eigenvalue of the original circuit, not only (16c) has to be satisfied, but also the additional conditions coming from (15c). This

means that the system

$$
\begin{pmatrix} \lambda C_k & 0 & -I & 0 \\ 0 & -I & 0 & \lambda L_k \\ B_{ck} & B_{lk} & 0 & 0 \\ 0 & 0 & \tilde{Q}_{ck} & \tilde{Q}_{lk} \end{pmatrix} \begin{pmatrix} v_{ck} \\ v_{lk} \\ i_{ck} \\ i_{lk} \end{pmatrix} = 0 \tag{18}
$$

must have a non-trivial solution for the same value of λ.

The coefficient matrix of (18) is a row-enlargement of that of (17), which as indicated above has generically corank one. If (18) has a non-trivial solution, the additional rows in (18) must be linearly dependent on those of (17) (always for generic values of C, L). Provided that the P-structure K is not a block, there is at least one additional row in the B_k rows of (18) coming from a hybrid loop. We know from the proof of Lemma 3 that this row cannot be expressed as a linear combination of the rows coming from $\tilde{B}_k$ only. Obviously, it cannot be written just in terms of the $\tilde{B}_k$ and $\tilde{Q}_k$ rows, either. Therefore, this linear dependence relation involves (some of) the C_k, L_k rows. Hence, if it is at all possible that system (18) has a non-vanishing solution, at least one algebraic restriction on the values of C_k and L_k must necessarily be met. We conclude that reactive values leading to PIEs, if any, must lie on a lower dimensional set.

Altogether, the reasoning above shows that, for a PIE associated with a given P-structure K which is not a block, either it must happen that the PIE is a multiple eigenvalue of the K-subcircuit (and this may happen only for values of L_k, C_k lying on a lower dimensional set), or at least one restriction on the values of these reactances imposed by the existence of a hybrid loop must be met. Since this holds for all P-structures, and there is only a finite number of them, the fact that none of them is a block restricts the possible values of inductances and capacitances to a finite union of lower dimensional sets, which obviously cannot fill the whole $\mathbb{R}_+^{b_c+b_l}$ space. This completes the proof of Theorem 2.

$\square$

4 RLC examples

Consider the two circuits displayed in Figure 1. None of the P-structures shown in Figure 2 is a block and, therefore, none of these circuits can be topologically non-hyperbolic, according to Theorem 2. In the sequel we use these circuits to illustrate the reasoning which supports this result. We believe that these examples should be of help for the reader to understand the discussion of Section 3. In particular, by means of the circuit on the left of Figure 1 we show how hybrid loops impose restrictions on the reactive values which yield PIEs, whereas the circuit on the right will be used to illustrate that multiple eigenvalues of the LC-subcircuit associated with a P-structure may lead to PIEs of the original circuit.

4.1 Example 1

Focus the attention on the circuit on the left of Figure 1. The LC-subcircuit defined by the P-structure is depicted in Figure 3.
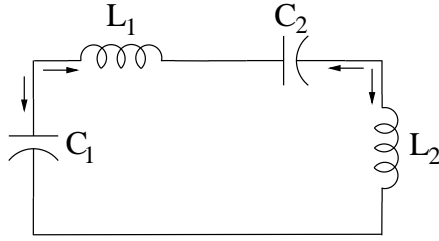
Figure 3: LC-subcircuit.

This is a tank circuit, with two capacitors and two inductors connected in series; the corresponding matrix pencil has a zero eigenvalue due to the presence of a C-cutset, an infinite eigenvalue due to the L-cutset, and a unique (hence simple) pair of purely imaginary eigenvalues given by

$$\lambda = \pm\sqrt{-\frac{C_1 + C_2}{C_1 C_2 (L_1 + L_2)}}. \tag{19}$$

Our aim is to illustrate how the hybrid loops in the full RLC circuit impose additional constraints on the reactive values which keep (19) as a PIE of the original circuit. The matrix arising in (17), which characterizes the eigenvalues of this LC-subcircuit, reads

$$\begin{pmatrix} \lambda C_1 & 0 & 0 & 0 & -1 & 0 & 0 & 0 \\ 0 & \lambda C_2 & 0 & 0 & 0 & -1 & 0 & 0 \\ 0 & 0 & -1 & 0 & 0 & 0 & \lambda L_1 & 0 \\ 0 & 0 & 0 & -1 & 0 & 0 & 0 & \lambda L_2 \\ 1 & 1 & -1 & -1 & 0 & 0 & 0 & 0 \\ 0 & 0 & 0 & 0 & 1 & 0 & 1 & 0 \\ 0 & 0 & 0 & 0 & 0 & 1 & 0 & 1 \\ 0 & 0 & 0 & 0 & 1 & 0 & 0 & 1 \end{pmatrix}. \tag{20}$$

In particular, the fifth row of this matrix arises from Kirchhoff's voltage law when applied to the LC-loop, whereas the sixth, seventh and eighth rows correspond to the current equations defined by the C_1-L_1, C_2-L_2 and C_1-L_2 cutsets of the LC-subcircuit.

Now, for the PIE (19) to be an eigenvalue of the original circuit, not only the homogeneous linear equations defined by (20) but also the additional ones arising in (18) must have a non-zero solution. These additional equations stem from the fact that the P-structure is not a block, and hence the hybrid loops will impose additional requirements. Two hybrid loops linearly independent of the LC-loop (cf. Figure 1) are defined by C_1, L_1, R_2 and C_1, L_2, R_1, respectively. They define two extra rows yielding non-zero entries within the $(B_c \; B_l)$ block of the coefficient matrix, namely

$$\begin{pmatrix} 1 & 0 & -1 & 0 & 0 & 0 & 0 & 0 \\ 1 & 0 & 0 & -1 & 0 & 0 & 0 & 0 \end{pmatrix}. \tag{21}$$

All but the fifth row of the matrix in (20) can be easily checked to be linearly independent. Hence, for (19) to be a PIE of the original circuit, the two rows of (21) must be linearly

dependent on those seven. Writing down the linear dependence relation for the first row, that is, for the first hybrid loop, and skipping computations for the sake of brevity, one gets the extra relation $\lambda = \pm\sqrt{-(L_1 C_1)^{-1}}$. Together with (19), this imposes the algebraic relation $L_1 C_1 = L_2 C_2$ as a necessary restriction for the existence of a PIE in the original circuit. Note that this is already enough to show in practice that the circuit cannot be topologically non-hyperbolic.

Proceeding analogously with the second row of (21), which comes from the second hybrid loop, we get the additional relation $L_1 C_2 = L_2 C_1$ and, together with the one above, we get $L_1 = L_2$, $C_1 = C_2$ as necessary relations for the existence of a PIE.

This is of course consistent with the results of [53]. Notice, however, that the approach there makes crucial use of the fact that this circuit has a unique LC-cutset. The use of P-structures overcomes this limitation and therefore extends the scope of [53].

4.2   Example 2

The circuit on the right of Figure 1 illustrates how multiple eigenvalues of the LC-subcircuit defined by a P-structure may well lead to PIEs in the original circuit. The P-structure depicted on the right of Figure 2 yields an LC-subcircuit defined by two independent tanks, as shown in Figure 4.
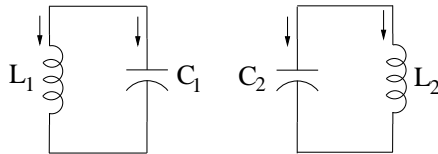

Figure 4: Double tank LC-subcircuit.

Certainly, the eigenvalues of this circuit are given by

$$\lambda_{1,2} = \pm\sqrt{-\frac{1}{L_1 C_1}}, \quad \lambda_{3,4} = \pm\sqrt{-\frac{1}{L_2 C_2}}, \tag{22}$$

which are simple if $L_1 C_1 \neq L_2 C_2$ and double if $L_1 C_1 = L_2 C_2$.

Proceeding as in Example 1, the reader can check that, under the assumption $L_1 C_1 \neq L_2 C_2$, none of these PIEs of the LC-subcircuit yield an eigenvalue of the original RLC circuit. By contrast, the assumption $L_1 C_1 = L_2 C_2$, which makes the PIE of the LC-circuit a double one, indeed leads to a PIE of the original circuit. In this case, this is a consequence of the fact that the double eigenvalue has index one and therefore the matrix (17) has corank two. Since no more than one hybrid loop (e.g. the one defined by the two capacitors and the two resistors) can be added to the LC-loops in a linearly independent manner, the matrix (18) will still be rank-deficient, showing that indeed the PIE will be an eigenvalue of the original circuit. As above, the results are consistent with the ones presented in [53], again without the need to use the fact that the circuit has a unique LC-cutset.

5 Circuits with mem-devices

We detail in this Section how to extend the results presented above to circuits including mem-devices, namely, memristors, memcapacitors and meminductors. These devices are being the object of much ongoing research in nonlinear circuit theory and electronics, not only from an analytical point of view [5, 14, 33, 41, 50, 54, 55] but also regarding applications in many different fields: see e.g. [29, 30, 43, 44, 45] and references therein.

5.1 Memristors, memcapacitors and meminductors

Circuit elements with memory (sometimes referred to as *mem-devices*) have been the object of a great attention in the last three years [14, 29, 30, 33, 41, 43, 44, 45, 50, 54, 55]. The origin of these devices can be found in Chua's 1971 paper [5]. For symmetry reasons, Chua postulated the existence of a nonlinear circuit element with a characteristic relating charge and flux, since resistors, capacitors and inductors already involved the current-voltage, voltage-charge and current-flux pairs. The report in 2008 of a nanometer device with a memristive characteristic (cf. [55]) had a great impact, and much research has been focused on this device since then. Memcapacitors and meminductors, introduced by Di Ventra *et al.* in [14], have also received considerable attention.

A memristor can be either charge-controlled or flux-controlled. The former has a characteristic of the form

$$\varphi = \phi(q),$$

whereas for the latter the constitutive relation reads as

$$q = \sigma(\varphi). \tag{23}$$

For the sake of simplicity we will focus the attention on flux-controlled memristors, although the results can be extended without difficulty to circuits including also charge-controlled ones. Differentiating the characteristic (23) and using the identities $q' = i$, $\varphi' = v$, one gets the current-voltage relation

$$i = W(\varphi)v, \tag{24}$$

where $W(\varphi) = \sigma'(\varphi)$ is the so-called *memductance*. This circuit element can be considered as a voltage-controlled resistor in which the conductance depends on $\varphi(t) = \int_{-\infty}^{t} v(\tau)d\tau$, thereby keeping track of the device history (hence the *memory resistor* or *memristor* name). In a charge-controlled setting the voltage-current relation has the form

$$v = M(q)i, \tag{25}$$

where $M(q) = \phi'(q)$ is the *memristance*. Note that both ϕ and σ must be actually nonlinear since otherwise the device would make no difference to a linear resistor.

Reactive elements with memory may be defined in a similar way. Specifically, a memcapacitor is governed by a relation of the form

$$q = C_m(\varphi)v, \tag{26}$$

so that the (mem-)capacitance C_m depends on $\varphi = \int v$. A meminductor is defined by

$$\varphi = L_m(q)i, \tag{27}$$

the (mem-)inductance L_m now depending on $q = \int i$. Find details in [14].

5.2 Circuit model and equilibria

The circuit model (1) may be expanded to accommodate also memristors, memcapacitors and meminductors, as detailed in what follows. As indicated above, for the sake of simplicity we assume the memristors to be flux-controlled. This yields the differential-algebraic model

$$
\begin{align}
C(v_c)v_c' &= i_c \tag{28a} \\
L(i_l)i_l' &= v_l \tag{28b} \\
\varphi_{mc}' &= v_{mc} \tag{28c} \\
q_{mc}' &= i_{mc} \tag{28d} \\
\varphi_{ml}' &= v_{ml} \tag{28e} \\
q_{ml}' &= i_{ml} \tag{28f} \\
\varphi_m' &= v_m \tag{28g} \\
0 &= B_c v_c + B_l v_l + B_{mc} v_{mc} + B_{ml} v_{ml} + B_r v_r + B_m v_m + B_j v_j + B_u v_s(t) \tag{28h} \\
0 &= Q_c i_c + Q_l i_l + Q_{mc} i_{mc} + Q_{ml} i_{ml} + Q_r i_r + Q_m i_m + Q_j i_s(t) + Q_u i_u \tag{28i} \\
0 &= q_{mc} - C_m(\varphi_{mc})v_{mc} \tag{28j} \\
0 &= \varphi_{ml} - L_m(q_{ml})i_{ml} \tag{28k} \\
0 &= i_r - \gamma(v_r) \tag{28l} \\
0 &= i_m - W(\varphi_m)v_m, \tag{28m}
\end{align}
$$

where the subscripts m, mc and ml correspond to memristors, memcapacitors and meminductors, respectively.

Equilibrium points are defined by the vanishing of the right-hand side of (28). It is easy to check that at equilibrium all voltages and currents in memristors, memcapacitors and meminductors are null, and so they are q_{mc} and φ_{ml} because of (28j)-(28k). In what follows we show how the results of Section 3 can be extended to the linearization of circuits with mem-devices at equilibria.

5.3 Linearization

In the linearization about any equilibrium point, one can check that the partial derivatives with respect to φ_m, φ_{mc} and q_{ml} of the map defining the right-hand side of (28) do vanish identically, because of the identities $v_m = 0$, $v_{mc} = 0$, $i_{ml} = 0$ at equilibrium. This means that the linearization displays a null eigenvalue whose geometric multiplicity equals the total number of mem-devices. The remaining eigenvalues are defined by the eigenvalue-eigenvector

equations

$$\lambda C v_c = i_c \tag{29a}$$

$$\lambda L i_l = v_l \tag{29b}$$

$$\lambda q_{mc} = i_{mc} \tag{29c}$$

$$\lambda \varphi_{ml} = v_{ml} \tag{29d}$$

$$0 = B_c v_c + B_l v_l + B_{mc} v_{mc} + B_{ml} v_{ml} + B_r v_r + B_m v_m \tag{29e}$$

$$0 = Q_c i_c + Q_l i_l + Q_{mc} i_{mc} + Q_{ml} i_{ml} + Q_r i_r + Q_m i_m \tag{29f}$$

$$0 = q_{mc} - C_m v_{mc} \tag{29g}$$

$$0 = \varphi_{ml} - L_m i_{ml} \tag{29h}$$

$$0 = i_r - G v_r \tag{29i}$$

$$0 = i_m - W v_m, \tag{29j}$$

obtained after short-circuiting voltage sources and open-circuiting current sources. Here C, L, C_m, L_m, G and W are the capacitance, inductance, memcapacitance, meminductance, conductance and memductance matrices at equilibrium. By means of a Schur reduction [28, 49] we may describe, via (29g)-(29h), the solutions of (29) in terms of those of

$$\lambda C v_c = i_c \tag{30a}$$

$$\lambda C_m v_{mc} = i_{mc} \tag{30b}$$

$$\lambda L i_l = v_l \tag{30c}$$

$$\lambda L_m i_{ml} = v_{ml} \tag{30d}$$

$$0 = B_c v_c + B_{mc} v_{mc} + B_l v_l + B_{ml} v_{ml} + B_r v_r + B_m v_m \tag{30e}$$

$$0 = Q_c i_c + Q_{mc} i_{mc} + Q_l i_l + Q_{ml} i_{ml} + Q_r i_r + Q_m i_m \tag{30f}$$

$$0 = i_r - G v_r \tag{30g}$$

$$0 = i_m - W v_m. \tag{30h}$$

The key remark is that, grouping together capacitors and memcapacitors, inductors and meminductors, and resistors and memristors, system (30) is formally identical to (6), in the understanding that C, L and G in (6) correspond in (30) to the block-diagonal matrices defined by C and C_m, L and L_m, and G and W, respectively. This fact supports Theorem 3 below, which is an analog of Theorem 2 for circuits with mem-devices. We denote by m the total number of memristors, memcapacitors and meminductors.

Theorem 3. *Assume that, at a given equilibrium, the matrices C, C_m, L, L_m are diagonal with positive entries, that G and W are positive definite, and that the circuit does not have either cutsets formed just by current sources and/or capacitors and/or memcapacitors or loops defined by voltage sources and/or inductors and/or meminductors. Disregarding m null eigenvalues associated with mem-devices, the circuit has a pair of purely imaginary eigenvalues for all positive values of capacitances, memcapacitances, inductances and meminductances if and only if, after open-circuiting current sources and short-circuiting voltage sources, the reduced circuit exhibits a capacitive-inductive block.*

Certainly, a capacitive-inductive block may now be composed of capacitors, memcapacitors, inductors and/or meminductors. As in the setting of Section 3, the block must include at least one capacitive and one inductive element for a PIE to exist.

5.4 Example 3

The circuit depicted in Figure 5 is proposed in [45] as a scheme to couple two quantum bits (cf. [11, 13, 42, 60]). Each qubit is defined by the series connection of a voltage source, a linear capacitor and a Josephson junction. The use of a memcapacitor is aimed at controlling the interaction between both qubits by pre-setting the value of the memcapacitance C_m. In what follows we examine how the presence of small memristive currents within the Josephson junctions affects the existence of purely imaginary eigenvalues in this circuit, and address certain related bifurcations.
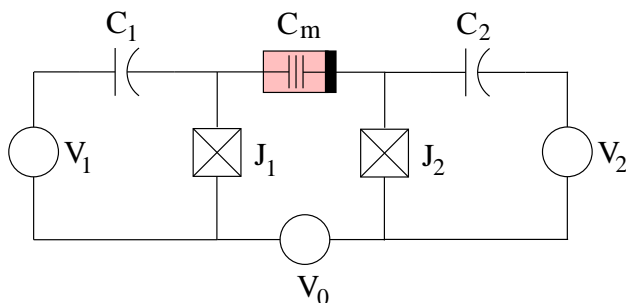

Figure 5: Memcapacitive coupling of two quantum bits.

The Josephson junction, which consists of two superconductors separated by an insulating layer, can be modelled as a nonlinear, flux-controlled inductor with a current-flux characteristic of the form

$$i_l = I_0 \sin(k_0 \varphi_l), \tag{31}$$

for certain physical constants I_0, k_0 [10]. Provided that $\cos(k_0 \varphi_l) \neq 0$, the incremental inductance is

$$L(\varphi_l) = \frac{1}{I_0 k_0 \cos(k_0 \varphi_l)}.$$

However, as detailed in [7], a small memristive current in parallel should also be taken into account in an accurate model of the Josephson junction. This memristive current is governed by

$$i_m = I_1 \cos(k_1 \varphi_m) v_m, \tag{32}$$

for certain constants I_1, k_1. The memductance reads as

$$W(\varphi_m) = I_1 \cos(k_1 \varphi_m).$$

Note that this expression may become negative for certain values of φ_m. We ignore other parasitic effects which are not relevant to our analysis. Replacing in Figure 5 both junctions by the parallel connection of a nonlinear inductor and a memristor governed by (31) and (32), respectively, we get the circuit depicted in Figure 6.
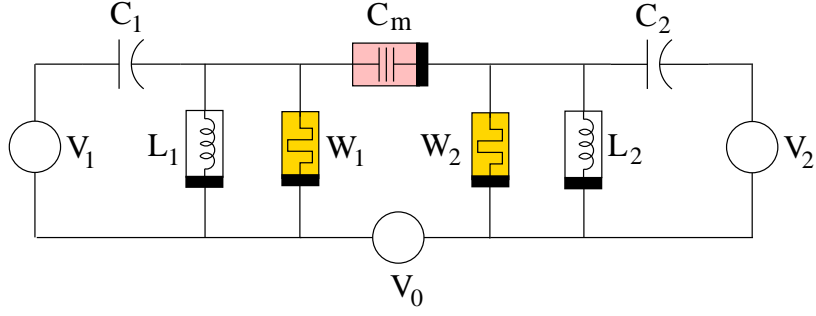
Figure 6: Equivalent circuit.

The uncoupled case, $C_m = 0$. Let us first consider the dynamics of the circuit displayed in Figure 6 when $C_m = 0$, that is, in the absence of the memcapacitor. In this situation both qubits are uncoupled and their dynamics can be analyzed independently. For notational simplicity, denote by V, C, L, W the DC voltage, capacitance, inductance and memductance of the (say) left qubit. The dynamics is defined by the model

$$
\begin{align}
Cv'_c &= I_0 \sin(k_0 \varphi_l) + W(\varphi_m)(V - v_c) \tag{33a} \\
\varphi'_l &= V - v_c \tag{33b} \\
\varphi'_m &= V - v_c. \tag{33c}
\end{align}
$$

Equilibria are defined by $v_c = V$ and $\sin(k_0 \varphi_l) = 0$, without restrictions on φ_m. Fix e.g. $\varphi_l = 0$, which yields a positive incremental inductance L in the Josephson junction. The linearization of (33) at this equilibrium can be easily checked to exhibit a null eigenvalue and a conjugate pair

$$
\lambda = \frac{-W}{2C} \pm \sqrt{\left(\frac{W}{2C}\right)^2 - \frac{1}{LC}}. \tag{34}
$$

No purely imaginary eigenvalues are displayed if $W \neq 0$. However, if $W = 0$ we get

$$
\lambda = \pm j \sqrt{\frac{1}{LC}}. \tag{35}
$$

This is a consequence of the fact that, ignoring memristive currents, each uncoupled qubit amounts to a (nonlinear) tank circuit after short-circuiting the voltage source, hence displaying a PIE in the linearized problem, as expected. Noteworthy, (34) can be seen as an unfolding of (35): when W becomes negative the pair of conjugate eigenvalues cross the imaginary axis towards the right half-plane and the equilibrium undergoes a Hopf bifurcation.

Our goal is to examine whether PIEs are also displayed in the presence of the memcapacitor when one memductance vanishes, and if our framework may shed some light in this regard. This task is undertaken below.

Memcapacitive coupling, $C_m \neq 0$. Let us drive our attention back to the circuit of Figure 6 with $C_m \neq 0$. Inspired on the discussion presented above for the case $C_m = 0$, one may conjecture if the vanishing of either W_1 or W_2 (but not both) is enough to support the existence of a pair of purely imaginary eigenvalues in the linearized circuit dynamics. As detailed later, checking whether this conjecture is true or not is by no means a trivial computation; it does not seem to have an easy response without the results discussed in this paper, either.

Assume e.g. that $W_1 > 0$, $W_2 = 0$. By short-circuiting the voltage sources, one gets the reduced circuit displayed in Figure 7.
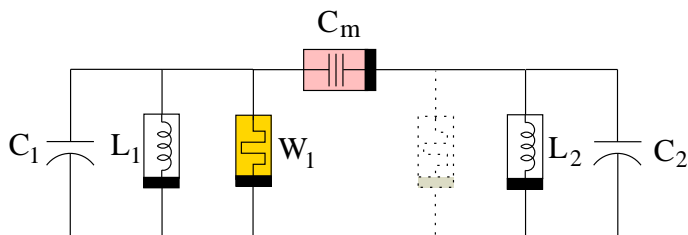

Figure 7: Reduced circuit with $W_2 = 0$.

Theorem 3 shows that the above conjecture is actually false if we seek for the existence of PIEs for arbitrary (albeit positive) values of C_m, C_i, L_i ($i = 1, 2$). This is a consequence of the fact that no capacitive-inductive block (in this case, a block composed of inductors, capacitors and/or the memcapacitor) is displayed in the reduced circuit. But our framework makes it possible to say more: the circuit has no PIEs for any single set of positive values of C_m, C_i, L_i if $W_1 > 0$, $W_2 = 0$. Indeed, a P-structure is needed for a PIE to be displayed, but the reduced circuit in Figure 7 has no P-structures. This claim can be checked as follows: all cutsets including C_1 or L_1 include also W_1, and therefore both C_1 and L_1 are precluded in any (tentative) P-structure. Such a P-structure should then involve L_2, C_2 and/or C_m, but the only loop within this set is the one defined by L_2 and C_2; they do not form a cutset, and the one that they define together with C_m involves the memcapacitor, which in turn does not form a loop just with C_2 and/or L_2. No P-structure may then support the existence of a PIE in the setting considered above, that is, if $W_1 > 0$, $W_2 = 0$; obviously, the same is true by symmetry if $W_1 = 0$, $W_2 > 0$.

It is not a simple task to compute the eigenvalues of the linearized dynamics in order to show in practice that no PIEs are displayed. In this case, the determinant of the matrix pencil characterizing the spectrum of the linearized problem can be written, for arbitrary values of C_m, C_i, L_i, W_i ($i = 1, 2$), as $\lambda^3 p(\lambda, z)$; for the sake of notational simplicity, we group together all the parameters C_m, C_1, C_2, L_1, L_2, W_1, W_2 into a single vector z. The triple zero owes to the two memristors and the memcapacitor, each one being responsible for a null eigenvalue. In turn, p can be written as

$$p(\lambda, z) = a_4\lambda^4 + a_3\lambda^3 + a_2\lambda^2 + a_1\lambda + a_0, \tag{36}$$

the coefficients of (36) being

$$
\begin{aligned}
a_4 &= kL_1L_2(C_1C_2 + C_1C_m + C_2C_m) \\
a_3 &= kL_1L_2((C_1 + C_m)W_2 + (C_2 + C_m)W_1) \\
a_2 &= k(L_1C_1 + L_2C_2 + (L_1 + L_2)C_m + L_1L_2W_1W_2) \\
a_1 &= k(L_1W_1 + L_2W_2) \\
a_0 &= k
\end{aligned}
$$

with $k = (L_1L_2C_1C_2)^{-1}$. The fact that a double PIE cannot exist is a simple consequence of the non-vanishing of a_3 and a_1 when $W_1 > 0$, $W_2 = 0$ and all inductances and capacitances are strictly positive. It is more difficult to rule out simple PIEs; we may in this case resort to the Routh-Hurwitz criteria for purely imaginary eigenvalues discussed in [35]. As detailed there, the existence of a simple PIE requires that the relation

$$
a_1^2 a_4 + a_0 a_3^2 - a_1 a_2 a_3 = 0 \tag{37}
$$

holds. The expression depicted in (37) can be written as a cubic polynomial in W_2 with coefficients depending on C_m, C_i, L_i, W_1; in particular, the independent term (the only one which does not necessarily vanish with W_2) is $k^3 L_1^3 L_2 C_m^2 W_1^2$. Provided that $W_1 > 0$, $W_2 = 0$, and that all inductances and capacitances are strictly positive, this expression cannot vanish and this confirms that, indeed, there are no simple PIEs.

Note that this kind of computation is not feasible for more complex problems, whereas our theoretical discussion reduces the analysis to a topological check in the circuit. The absence of PIEs if both W_1 and W_2 are strictly positive can be derived from our framework in a similar way. Finally, if both W_1 and W_2 vanish, then the whole reduced circuit is a capacitive-inductive block and the existence of PIEs for arbitrary positive values of C_m, C_i and L_i follows.

6 Concluding remarks

In this paper we have characterized topologically non-hyperbolic configurations in strictly passive circuits, yielding purely imaginary eigenvalues for *all* values of the capacitances and inductances. Our approach captures explicitly the circuit topology by means of branch-oriented DAE models. The use of so-called P-structures makes it possible to extend the scope of our framework beyond the setting considered in [53], which only applies to circuits with a unique LC-loop or a unique LC-cutset. Additionally, we have shown how to accommodate mem-devices (namely, memristors, memcapacitors and meminductors) in the hyperbolicity analysis. Several examples illustrate our results.

References

[1] B. Andrásfai, *Graph Theory: Flows, Matrices,* Adam Hilger, 1991.

[2] B. Bollobás, *Modern Graph Theory*, Springer-Verlag, 1998.

[3] A. Boukabou, B. Sayoud, H. Boumaiza and N. Mansouri, Control of n-scroll Chua's circuit, *Internat. J. Bifurcation and Chaos* **19** (2009) 3813-3822.

[4] A. Buscarino, L. Fortuna and M. Frasca, Jump resonance in driven Chua's circuit, *Internat. J. Bifurcation and Chaos* **19** (2009) 2557-2561.

[5] L. O. Chua, Memristor – The missing circuit element, *IEEE Trans. Circuit Theory* **18** (1971) 507-519.

[6] L. O. Chua, Dynamic nonlinear networks: state-of-the-art, *IEEE Trans. Circuits and Systems* **27** (1980) 1059-1087.

[7] L. O. Chua, Nonlinear circuit foundations for nanodevices, Part I: The four-element torus, *Proc. IEEE* **91** (2004) 1830-1859.

[8] L. O. Chua and A. D. Deng, Impasse points, I: Numerical aspects, *Internat. J. Circuit Theory Appl.* **17** (1989) 213-235.

[9] L. O. Chua and A. D. Deng, Impasse points, II: Analytical aspects, *Internat. J. Circuit Theory Appl.* **17** (1989) 271-282.

[10] L. O. Chua, C. A. Desoer and E. S. Kuh, *Linear and Nonlinear Circuits*, McGraw-Hill, 1987.

[11] A. Csurgay, On circuit models for quantum-classical networks, *Internat. J. Circuit Theory Appl.* **35** (2007) 471-484.

[12] A. Demir, Floquet theory and non-linear perturbation analysis for oscillators with differential-algebraic equations, *Internat. J. Circuit Theory Appl.* **28** (2000) 163-185.

[13] M. H. Devoret, A. Wallraff and J. M. Martinis, Superconducting qubits: A short review, preprint, 2004; http://arxiv.org/abs/cond-mat/0411174.

[14] M. Di Ventra, Y. V. Pershin and L. O. Chua, Circuit elements with memory: memristors, memcapacitors and meminductors, *Proc. IEEE* **97** (2009) 1717-1724.

[15] D. Estévez-Schwarz and C. Tischendorf, Structural analysis of electric circuits and consequences for MNA, *Internat. J. Circuit Theory Appl.* **28** (2000) 131-162.

[16] M. Fosséprez, *Non-Linear Circuits: Qualitative Analysis of Non-linear, Non-Reciprocal Circuits*, John Wiley & Sons, 1992.

[17] L. R. Foulds, *Graph Theory Applications*, Springer, 1992.

[18] E. Freire, E. Ponce and J. Ros, Following a saddle-node of periodic orbits' bifurcation curve in Chua's circuit, *Internat. J. Bifurcation and Chaos* **19** (2009) 487-495.

[19] G. Gandhi and T. Roska, MOS-integrable circuitry for multi-scroll chaotic grid realization: A SPICE-assisted proof, *Internat. J. Circuit Theory Appl.* **37** (2009) 473-483.

[20] F. R. Gantmacher, *The Theory of Matrices,* vol. 2, Chelsea, 1959.

[21] M. M. Green and A. N. Willson Jr, An algorithm for identifying unstable operating points using SPICE, *IEEE Trans. on Computer-Aided Design of Circuits and Systems* **14** (1995) 360-370.

[22] M. Günther and U. Feldmann, CAD-based electric-circuit modeling in industry. I: Mathematical structure and index of network equations, *Surv. Math. Ind.* **8** (1999) 97-129.

[23] M. Günther and U. Feldmann, CAD-based electric-circuit modeling in industry. II: Impact of circuit configurations and parameters, *Surv. Math. Ind.* **8** (1999) 131-157.

[24] S. S. Gupta, R. K. Sharma, D. R. Bhaskar and R. Senani, Sinusoidal oscillators with explicit current output employing current-feedback op-amps, *Internat. J. Circuit Theory Appl.* **38** (2010) 131-147.

[25] B. C. Haggman and P. R. Bryant, Geometric properties of nonlinear networks containing capacitor-only cutsets and/or inductor-only loops. Part I: Conservation laws, *Cir. Sys. Signal Process.* **5** (1986) 279-319.

[26] B. C. Haggman and P. R. Bryant, Geometric properties of nonlinear networks containing capacitor-only cutsets and/or inductor-only loops. Part II: Symmetries, *Cir. Sys. Signal Process.* **5** (1986) 435-448.

[27] M. Hasler and J. Neirynck, *Nonlinear Circuits*, Artech House, 1986.

[28] R. A. Horn and Ch. R. Johnson, *Matrix Analysis,* Cambridge Univ. Press, 1985.

[29] M. Itoh and L. O. Chua, Memristor oscillators, *Internat. J. Bifurcation and Chaos* **18** (2008) 3183-3206.

[30] M. Itoh and L. O. Chua, Memristor cellular automata and memristor discrete-time cellular neural networks, *Internat. J. Bifurcation and Chaos* **19** (2009) 3605-3656.

[31] H. H. C. Iu, A. L. Fitch and D. Yu, Chaos in a twin-T circuit, *Internat. J. Bifurcation and Chaos* **20** (2010), in press.

[32] S. Jafari, M. Haeri and M. S. Tavazoei, Experimental study of a chaos-based communication system in the presence of unknown transmission delay *Internat. J. Circuit Theory Appl.* **38** (2010) 1013-1025.

[33] O. Kavehei, A. Iqbal, Y. S. Kim, K. Eshraghian, S. F. Al-Sarawi and D. Abbott, The fourth element: characteristics, modelling and electromagnetic theory of the memristor, *Proc. Royal Soc. A* **466** (2010) 2175-2202.

[34] C. Letellier and J. M. Ginoux, Development of the nonlinear dynamical systems theory from radio engineering to electronics, *Internat. J. Bifurcation and Chaos* **19** (2009) 2131-2163.

[35] W. M. Liu, Criterion of Hopf bifurcations without using eigenvalues, *J. Math. Anal. Appl.* **182** (1994) 250-256.

[36] A. C. J. Luo and B. Xue, An analytical prediction of periodic flows in the Chua circuit system, *Internat. J. Bifurcation and Chaos* **19** (2009) 2165-2180.

[37] R. N. Madan, *Chua's Circuit: A Paradigm for Chaos*, World Scientific, 1993.

[38] I. Manimehan, K. Thamilmaran and P. Philominathan, Enriched dynamics of a simple nonlinear nonautonomous parallel LCR circuit, *Internat. J. Bifurcation and Chaos* **19** (2009) 2347-2358.

[39] T. Matsumoto, L. O. Chua and A. Makino, On the implications of capacitor-only cutsets and inductor-only loops in nonlinear networks, *IEEE Trans. Circuits and Systems* **26** (1979) 828-845.

[40] A. I. Mees and L. O. Chua, The Hopf bifurcation theorem and its applications to nonlinear oscillations in circuits and systems, *IEEE Trans. Circuits and Systems* **26** (1979) 235-254.

[41] B. Muthuswamy, Implementing memristor based chaotic circuits, *Internat. J. Bifurcation and Chaos* **20** (2010) 1335-1350.

[42] M. A. Nielsen and I. L. Chuang, *Quantum Computation and Quantum Information*m, Cambridge Univ. Press, 2000.

[43] Y. V. Pershin and M. Di Ventra, Practical approach to programmable analog circuits with memristors, *IEEE Trans. Circuits and Systems I* **57** (2010) 1857-1864.

[44] Y. V. Pershin and M. Di Ventra, Experimental demonstration of associative memory with memristive neural networks, *Neural Networks* **23** (2010) 881-886.

[45] Y. V. Pershin and M. Di Ventra, Neuromorphic, digital and quantum computation with memory circuit elements, preprint, 2010; http://arxiv.org/abs/1009.6025. *Proc. IEEE* (submitted).

[46] P. C. Rech and H. A. Albuquerque, A hyperchaotic Chua system, *Internat. J. Bifurcation and Chaos* **19** (2009) 3823-3828.

[47] T. Reis, Circuit synthesis of passive descriptor systems - a modified nodal approach, *Internat. J. Circuit Theory Appl.* **38** (2010) 44-68.

[48] G. Reiszig, Differential-algebraic equations and impasse points, *IEEE Trans. Circuits and Systems I* **43** (1996) 122-133.

[49] R. Riaza, *Differential-Algebraic Systems. Analytical Aspects and Circuit Applications*, World Scientific, 2008.

[50] R. Riaza, Nondegeneracy conditions for active memristive circuits, *IEEE Transactions on Circuits and Systems II* **57** (2010) 223-227.

[51] R. Riaza, Graph-theoretic characterization of bifurcation phenomena in electrical circuit dynamics, *Internat. J. Bifurcation and Chaos* **20** (2010) 451-465.

[52] R. Riaza and C. Tischendorf, Qualitative features of matrix pencils and DAEs arising in circuit dynamics, *Dynamical Systems* **22** (2007) 107-131.

[53] R. Riaza and C. Tischendorf, The hyperbolicity problem in electrical circuit theory, *Math. Methods Appl. Sciences* **33** (2010) 2037-2049.

[54] R. Riaza and C. Tischendorf, Semistate models of electrical circuits including memristors, *Internat. J. Circuit Theory Appl.*, accepted, in press, 2011.

[55] D. B. Strukov, G. S. Snider, D. R. Stewart and R. Stanley Williams, The missing memristor found, *Nature* **453** (2008) 80-83.

[56] M. Tadeusiewicz, Global and local stability of circuits containing MOS transistors, *IEEE Trans. Circuits and Systems I* **48** (2001) 957-966.

[57] M. Takamatsu and S. Iwata, Index characterization of differential-algebraic equations in hybrid analysis for circuit simulation, *Internat. J. Circuit Theory Appl.* **38** (2010) 419-440.

[58] C. Tischendorf, Topological index calculation of DAEs in circuit simulation, *Surv. Math. Ind.* **8** (1999) 187-199.

[59] S. Yu, W. K. S. Tang, J. Lü and G. Chen, Generating $2n$-wing attractors from Lorenz-like systems, *Internat. J. Circuit Theory Appl.* **38** (2010) 243-258.

[60] A. Zagoskin and A. Blais, Superconducting qubits, *La Physique au Canada* **63** (2007) 215-227; http://arxiv.org/abs/0805.0164.

[61] Z. Zhang, G. Chen and S. Yu, Hyperchaotic signal generation via DSP for efficient perturbations to liquid mixing, *Internat. J. Circuit Theory Appl.* **37** (2009) 31-41.